Molecular Crystals and Liquid Crystals Science and Technology. Section A. Molecular Crystals and Liquid Crystals

Publication details, including instructions for authors and subscription information:
http://www.tandfonline.com/loi/gmcl19

New Chiral Tolane Series with Antiferroelectric Properties

P. Cluzeau [a], H. T. Nguyen [a], C. Destrade [a], N. Isaert [b], P. Barois [a] & A. Babeau [a]

[a] Centre de Recherche Paul Pascal Avenue A. Schweitzer, F33600, Pessac Cedex, France

[b] Laboratoire de Dynamique et Structure des Matériaux Moléculaires, Université de Lillel, F59655, Villeneuve d'Ascq Cedex, France

Version of record first published: 23 Sep 2006.

To cite this article: P. Cluzeau , H. T. Nguyen , C. Destrade , N. Isaert , P. Barois & A. Babeau (1995): New Chiral Tolane Series with Antiferroelectric Properties, Molecular Crystals and Liquid Crystals Science and Technology. Section A. Molecular Crystals and Liquid Crystals, 260:1, 69-91

To link to this article: http://dx.doi.org/10.1080/10587259508038684

Mol. Cryst. Liq. Cryst. 1995, Vol. 260, pp. 69–91
Reprints available directly from the publisher
Photocopying permitted by license only

NEW CHIRAL TOLANE SERIES WITH ANTIFERROELECTRIC PROPERTIES

P. CLUZEAU, H. T. NGUYEN, C. DESTRADE, N. ISAERT*, P. BAROIS, A. BABEAU.

Centre de Recherche Paul Pascal
Avenue A. Schweitzer
F33600 Pessac Cedex, France

*Laboratoire de Dynamique et Structure des Matériaux Moléculaires,
Université de Lille1
F59655 Villeneuve d'Ascq Cedex, France

Abstract: A new series of chiral tolane with aliphatic end chains ranging from heptyloxy to dodecyloxy has been synthesized and characterized. The mesomorphic properties have been analyzed by optical microscopy on pure compounds and mixtures, D.S.C , electro-optical and pitch measurements. This series displays a very rich polymesomorphism including S_A, $S_{C^*\alpha}$,S_{C^*}, S_{C^*FI}, S_{C^*A}, S_{I^*A} and S_{J^*} phases with reference to the compound MHPOBC through miscibility test. One of the characteristic of this serie is the two S_{C^*FI} phases (S_{C^*FI1} and S_{C^*FI2}) between S_{C^*} and S_{C^*A} phases. The electro-optical measurements were carried out with the classical SSFLC geometry. The threshold field is measured in each tilted mesophase; this one is peculiarly high in S_{J^*}, S_{I^*A} and S_{C^*A} phase (respectively more than 6; 4 and 1V/μm). In the S_{C^*FI} phase one can note a first plateau between 0.3V/μm an 0.7V/μm, and the saturation is reached at 1V/μm. Helical pitch measurement shows a strong variation of the pitch at the S_{C^*A}-S_{C^*FI} and S_{C^*FI}-S_{C^*} transitions.

I INTRODUCTION

During the last five years chiral liquid crystals have been paid much attention with the experimental discovery of the twist grain boundary phase (TGB) by Goodby et al[1] and the smectic C antiferroelectric phase by Chandani et al[2] in 1989. The research on the TGB phase is of fundamendal interest, on the other hand the studies of the S_{C^*} ferro, ferri and antiferroelectric phases are not only structural but also for device applications. Recently, Fukuda et al in a review[3], mentionned that up to now there are more than 300 pure compounds which display these properties. The structure of the

S_C^* ferro and antiferroelectric is well established but that of the $S_C^*F_I$ and $S_C^*\alpha$ is not too clear. In these investigated materials, the temperature range of these two last phases is too short and their careful studies are difficult. For these reasons, the search of new materials is always welcome. This paper presents a detailed analysis of a new chiral series with a tolane core having the general formula:

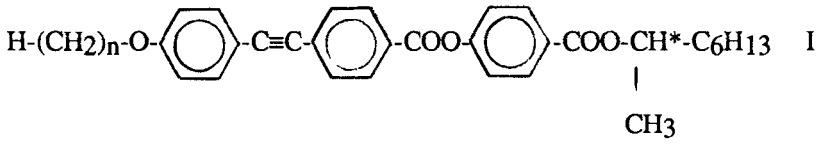

I

where n=7-12

II SYNTHESIS

The compounds studied in this paper are prepared following the schemes

Scheme 1

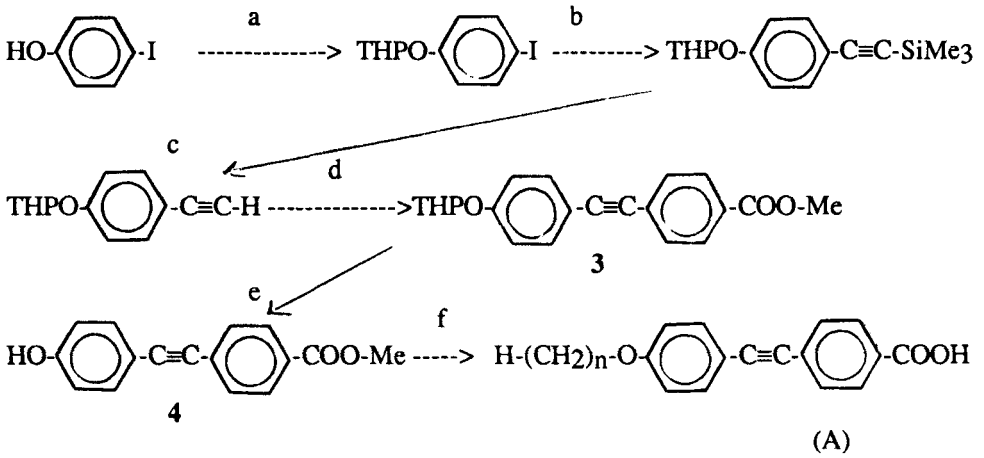

a) DHP, PTSA, CH_2Cl_2; b) $HC{\equiv}C\text{-}SiMe_3$, $PdCl_2$, $Cu(AcO)_2;H_2O$, Pr_2NH

c) NaOH 50%, MeOH, THF; d) $I\text{-}C_6H_4\text{-}COOMe$, $PdCl_2$, $Cu(AcO)_2;H_2O$, Pr_2NH

e) PTSA, THF, MeOH; f) $C_nH_{2n+1}\text{-}Br$, KOH, EtOH; HCl, H_2O

Scheme 2

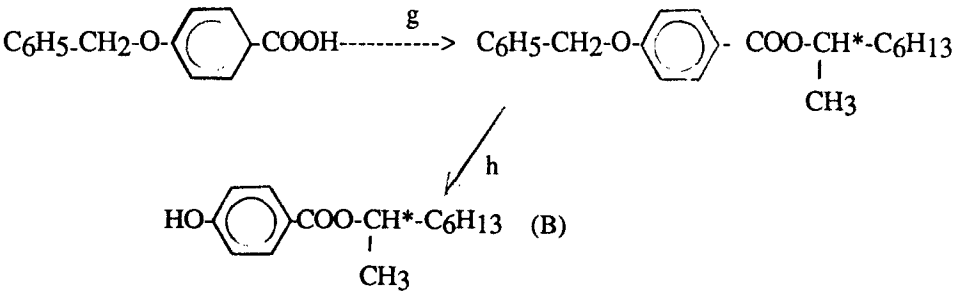

g) (S)-2-octanol, DCC, DMAP, CH_2Cl_2; h) H_2, Pd/C, EtOH

Scheme 3

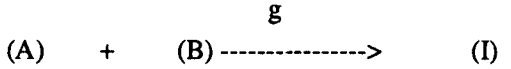

III MESOMORPHIC PROPERTIES

All of the compounds are mesogenic. The phase behaviour and transition temperatures of the series were determined both by thermal microscopy (Mettler FP5) and by differential scanning calorimetry (Perkin-Elmer DSC7). The liquid crystal transition temperatures and enthalpies for these new materials are summarized in Table 1.

* The S_A phase is observed in all the series from n=7 to n=12. Its temperature range decreases with the chain length. The classical optical texture is focal conic or homeotropic, but with a good planar alignment it displays some long focal conic defects (Figure 1a)

*The $S_C^*\alpha$ phase is present in three first compounds (n=7-9). It is identified only in good planar alignment with long parallel defects (Figure 1b).

*The S_C^* is obtained in all the materials. Its thermal stability increases with the chain length. It differencies the other phases by broken fan shaped textures or pseudo homeotropic domains but with the same sample it resembles to "corn-rod" (Figure 1c).

* The S_C^*FI phase is always obtained between S_C^* and S_C^*A phases and only observedwith homeotropic alignment . The S_C^*-S_C^*FI and S_C^*FI-S_C^*A transitions display some thermal fluctuation due to helical pitch change.In many compounds, we detected two different S_C^*FI phases having the same textures and the same behaviour

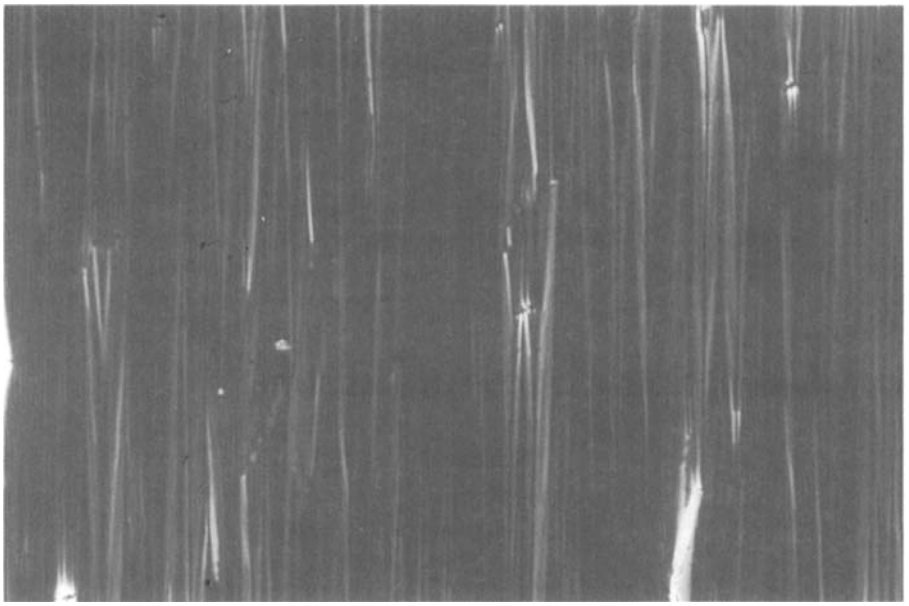

Figure 1a: Optical texture of S_A phase at 109°C of n=9.

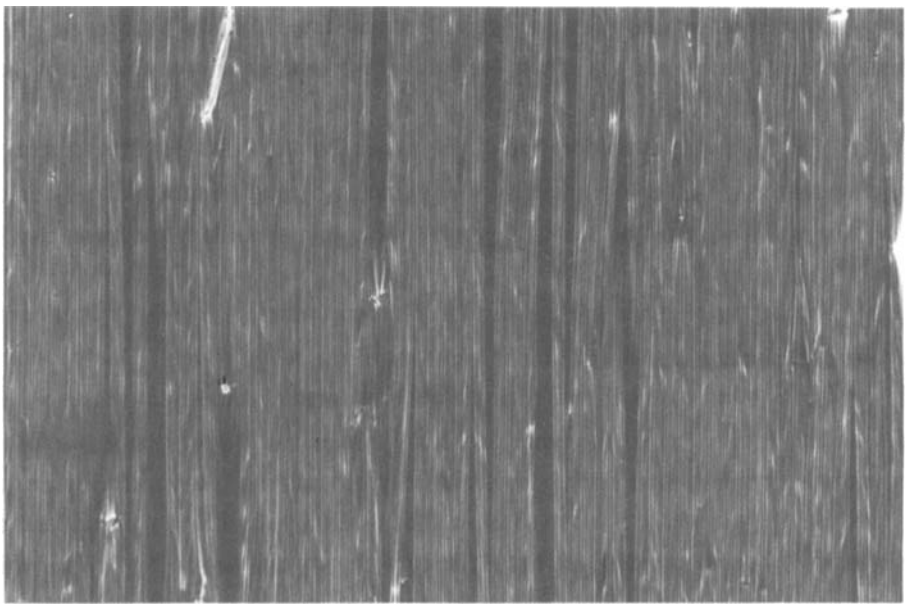

Figure 1b: Optical texture of $S_C{}^*\alpha$ phase at 108.1°C of n=9. See Color Plate VI.

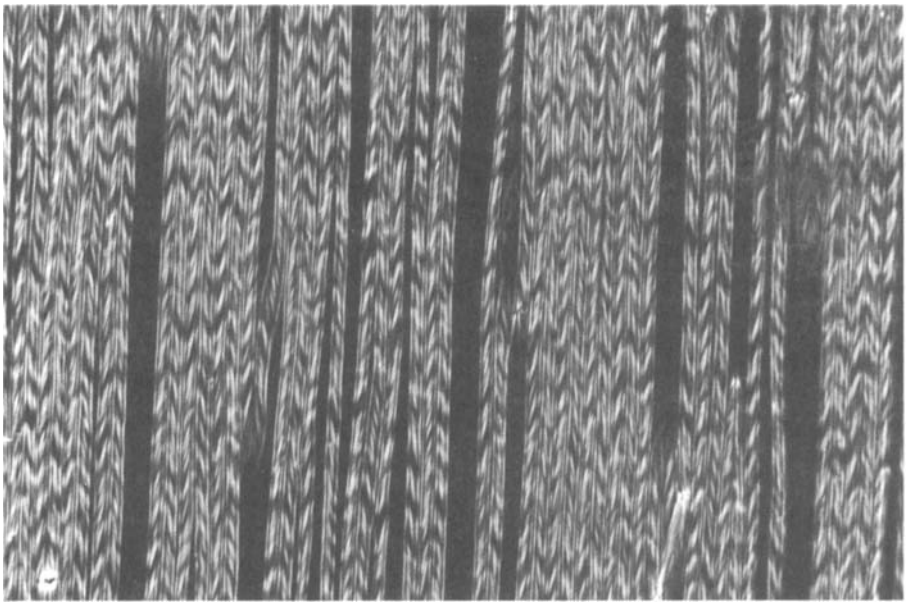

Figure 1c: Optical texture of $S_{C}*$ phase at 105°C of n=9.

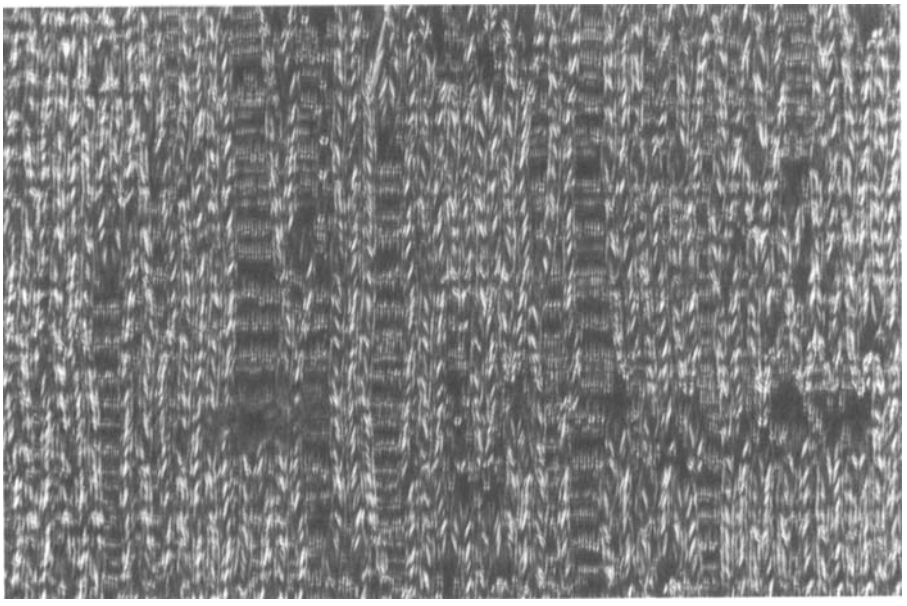

Figure 1d: Optical texture of $S_{C}*_{A}$ phase at 85°C of n=9.
See Color Plate VI continued.

on electro-optical studies (next paragraph). The DSC shows clarely their existence between S_C^* and S_{C^*A} phases (Figure 2).

* The S_{C^*A} phase has the same texture than the S_C^* phase but with this sample one can see some additional defects perpendicular (Figure 1d).

Table 1: Transition temperatures (°C) and enthalpies in italic (KJ/mol^{-1}) of I

n	K	S_{C^*A}	S_{C^*FI1}	S_{C^*FI2}	S_{C^*}	$S_{C^*\alpha}$	S_A	I
7 *	92.3	(87.5)	(88.3)	(90)	96.1	98.4	136	
8 *	67.6	95.1	96	97	104	105.5	135.3	
9 *	62.2 *22.1*	92.5 *0.009*	95 *0.024*	-	107.6 *0.27*	108.5	129.6 *3.2*	
10	58.2	94.6	96.1	-	111.2	-	128.6	
11	66 *32.6*	89 *0.01*	92.3 0.019	-	112.4 *0.45*	-	123 *2.2*	
12	73.4	92	94.3	-	113.2		121.3	

* For n=7,8,9 there is an S_J^* and S_{I^*A} phases between K and S_{C^*A} phase:

n	K	S_J^*	S_{I^*A}	S_{C^*A}
7	92.3	(69.6)	(73.7)	
8	67.6	(65)	71.6	
9	62.2 *22.1*	(56) *0.023*	64 *2.6*	

The above assignment of the different smectic phases relies mainly on the miscibility diagram between the C8 tolane and the well known MHPOBC compound[1] shown in figure 3. This study is similar to that observed by Heppke et al

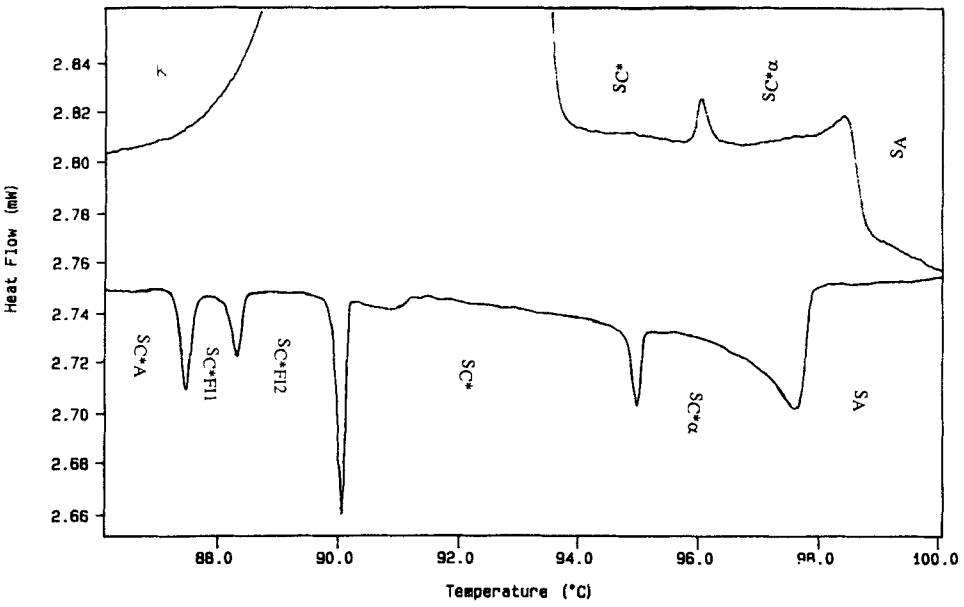

Figure 2: DSC thermogram of n=7

IV ELECTROOPTIC PROPERTIES

The material was confined between two ITO coated glass slides, the active area is 0.25 cm^2. To achieve a planar alignement the glasses were covered with a rubbed polyamid layer. The thickness of the cell used was 5 and 7.5 µm (purchased from Linkam L.T.D). The alignement was improved by very slow cooling through the isotropic to S_A phase transition (0.1°C/mn).

A classical electrooptical set up was used to the mesurement of both switching current, electric response time and apparent tilt angle[5].

With this serie of molecules, once the samples have been oriented, the alignement remains good even after several crystallisations.

1/ Polarisation, electric response time and tilt angle at saturation versus temperature

The spontaneous polarisation is calculated by integration of switching current under a rectangular ac field at 15 Hz. The field value is 5V/µm, such a field is

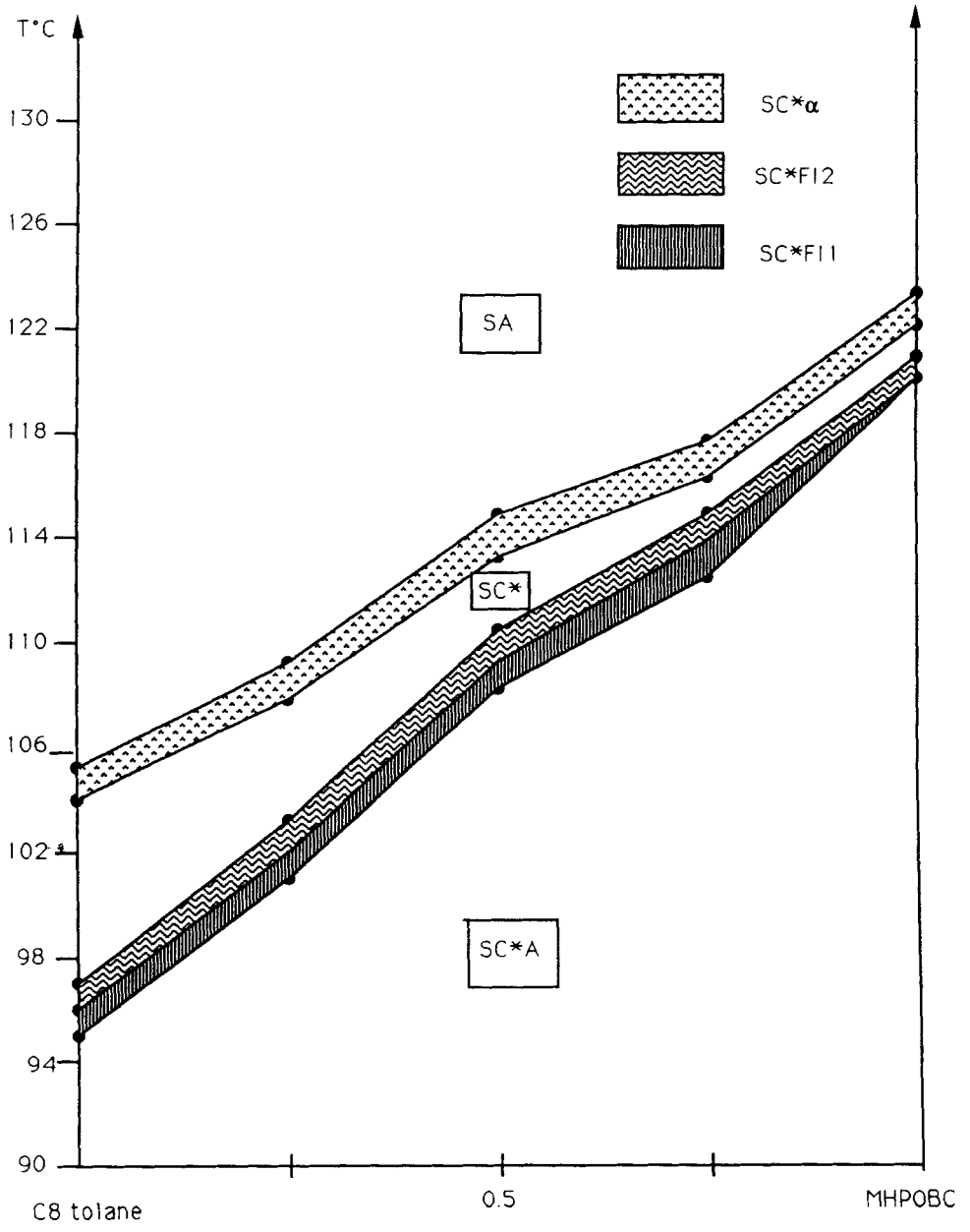

Figure 3: Isobaric phase diagram showing the isomorphy of the phases of the tolane (n=8) with those of MHPOBC.

sufficient to unwind the helical structure and to accomplish the phase transition from S_C^*A, S_C^*FI, S_C^*, $S_C^*\alpha$ phases to unwound SC* phase.

As picture in figure 4 the polarisation versus temperature shows no anomalies at the phase transition temperatures.

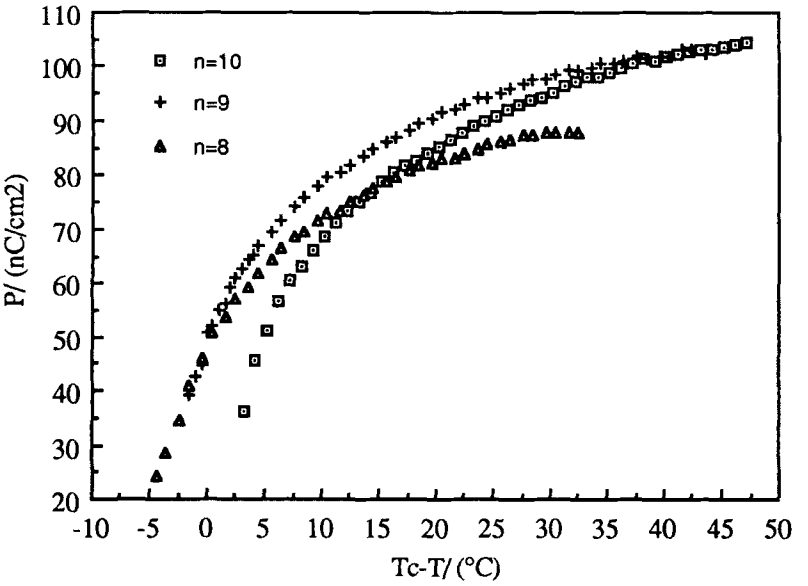

Figure 4: Temperature dependence of the polarisation at saturation (E=5 V/μm) for n=8,9,10. (Tc: transition temperature between S_A phase and tilted smectic phase)

For n=8 and n=9 polarisation is still measurable a few degrees after $S_C^*\alpha\_S_A$ transition; This experimental fact could be explained by an important electroclinic effect. Whereas for n=10 electroclinic contribution near $S_C^*\_S_A$ transition should be very small, indeed the polarisation can not be measure a few degrees before $S_C^*\_S_A$ transition. This behaviour very different between n=10 and n=8,9 suggest that a large electroclinic contribution in S_A phase is connected with the existence of $S_C^*\alpha$ phase. We note that the polarisation is bigger for long chain; this fact is unusual (generaly the polarisation increase when the length of the chain decrease), but perfectly coherent with the tilt angle value (25° for n=8; 28.5° for n=9 and 31° for n=10).

Electric response time is defined as the time between field reversion and the maximum of the polarisation pic. This measurement is realised at the same time as

polarisation measurement. Obviously the electric response time decrease by increasing temperature (see figure 5)

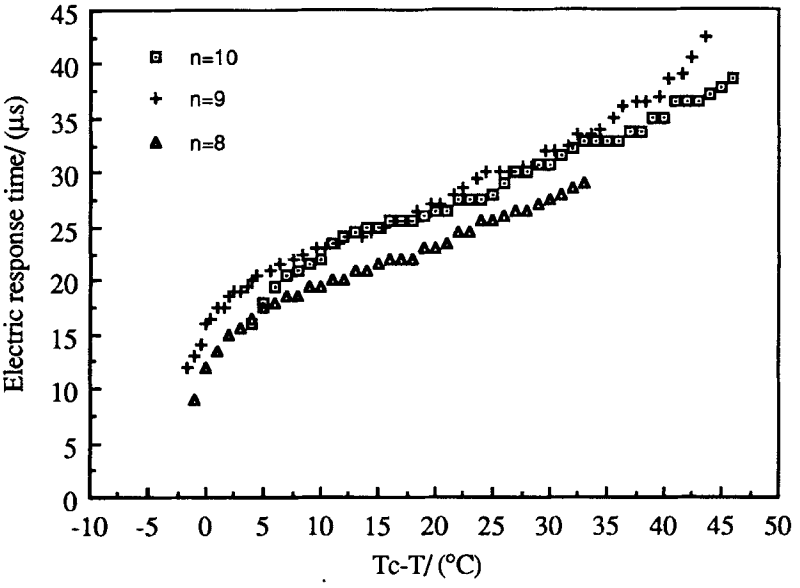

Figure 5:Temperature dependence of the electric response time at saturation (E=5V/μm) for n=8,9,10.(Tc: transition temperature between S_A phase and tilted smectic phase)

On the other hand the electric response time is smaller for n=8 even if the polarisation is smaller for n=8 (τ is proportionnal to γ/PE); this fact show that the viscosity parameter is predominant.

The apparent tilt angle θ of molecules from the smectic layer normal was calculated from the difference between extinction positions of the sample between crossed polarizers under rectangular ac field (4V/μm) at very low frequency (0.2Hz). The accuracy of the measurement was estimated at ±1°.

As for polarisation tilt angle versus temperature shows no anomalies at the phase transition temperature (see figure 6); this is consistent with the value of the field at which the switch concern only the two ferroelectric states. We note that the variation of the apparent tilt angle in S_C*_A phase are weak (respectively 4°,1°and 2.5° for n=8,9,10). Furthermore we observed exactly the same behaviour for the tilt angle versus temperature than polarisation: indeed tilt angle in S_A phase is important only on n=8,9 (compound with S_C*_α) and not on n=10.

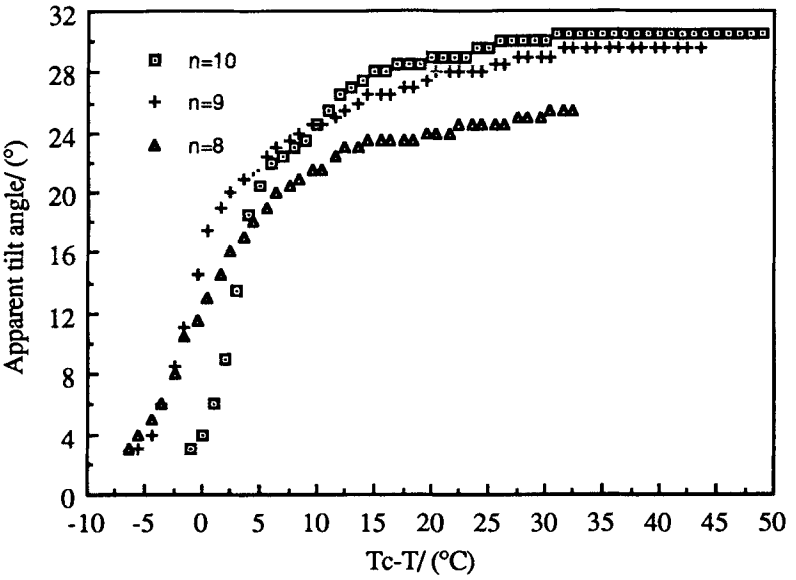

Figure 6:Temperature dependence of the apparent tilt angle at saturation (E=5V/μm) for n=8,9,10.(Tc: transition temperature between S_A phase and tilted smectic phase)

2/ Behaviour versus field in S_J*, S_I*A, S_C*A, S_C*FI, S_C* phases

The study of the behaviour versus field in S_C*A, S_C*FI, S_C* phases are given only for n=10 compound except obviously for S_J* and S_I*A (compound n=8).

S_C* phase

We have not been able to get any accurate measurement in the S_C*α phase owing to very short temperature range. On the contrary in the SC* phase the behaviour under electric field is very classical, namely polarisation saturation is rapidly reached with a low field (see figure 7).

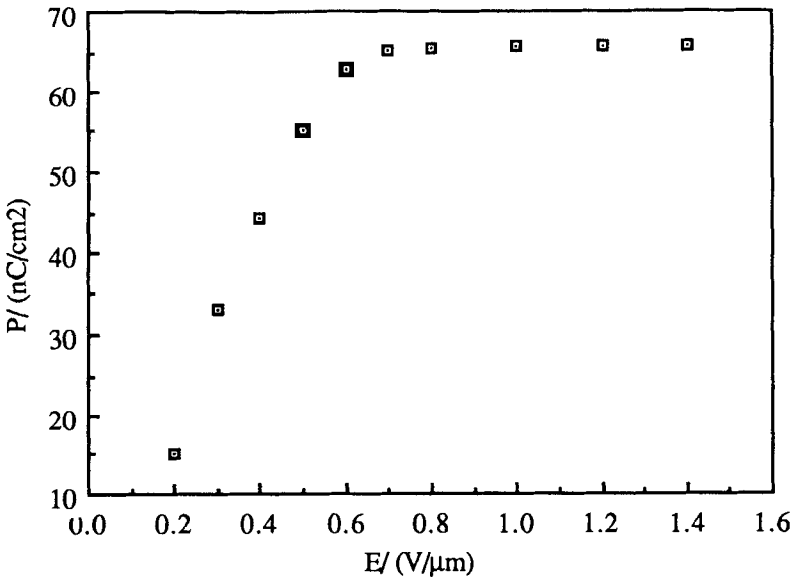

Figure 7: Polarisation versus field in S_C^* phase at 100°C for n=10. (7.5 μm thick sample)

S_C^*FI phase

The structures of S_C^*FI phases are not experimentally established, but several models have been proposed.

All these models are more or less consistent with the experimental facts showing at least the local dipole moment is partially compensated[6,7,8].

In S_C^*FI phase the behaviour of polarisation versus the field is rather peculiar: at low field there is a step approximatively at Ps/2 (see figure 9). This fact occurs for all studied material in this serie (n=8,9,10) and also for another series exhibiting a S_C^*FI phase[9]. Moreover the value of this step (P/2) is independent of the thickness of the sample although the lenght of the step increase a little with the thickness of the sample. Nevertheless there is no experimental difference betwen material exhibiting two ferrielectric phases (n=8) or one (n=10). This step is certainly a ferrielectric state with is close to the behaviour of the apparent tilt angle versus electric field in ferrielectric phase[10].

Furthermore there is certainly a link between this ferrielectric state at low field and conoscopic observation, indeed conoscopic observation at low field shows the optic

plane to be parallel to the field direction which corresponds to the polarisation perpendicular to the electric field[6,7,8].

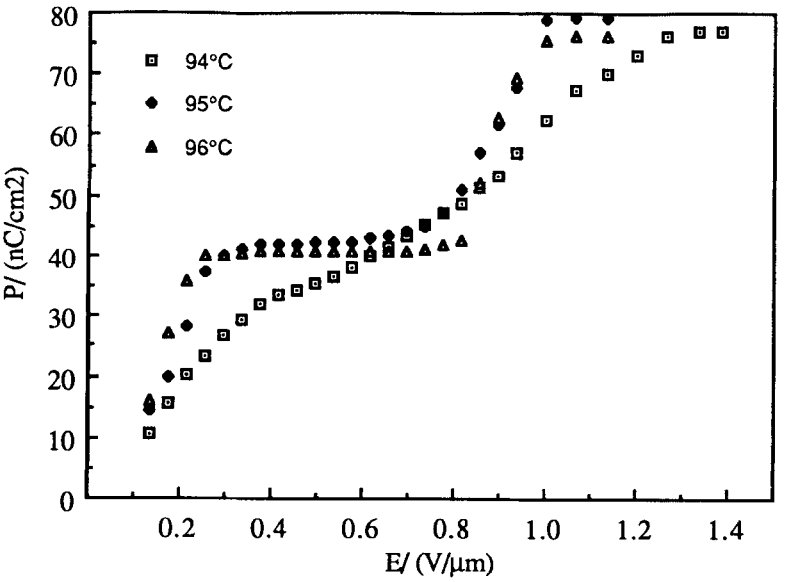

Figure 9: Polarisation versus field in SC*FI phase at 94, 95 and 96°C for n=10; 94°C is just below SC*A/SC*FI transition. (7.5 μm thick sample)

SC*A phase

In SC*A phase the molecules are organized in a herringbone fashion[11,12] (the dipole moment is compensated to zero on a microscopic scale). Namely the SC*A phase is chiral SC* phase where the molecules in the neighbouring layer normal are tilted in the opposite directions (as it shows by free standing film[13]) therefore, the local polarisation is vanishing in two successive layers.

All experimental results are consistent with this structure: the three stable switching state, zero electrooptic response at low field and a non polar behaviour of the conoscopic figure in an electric field[7].

As a consequence the SC*A phase require an important field to accomplish transition to ferroelectric phase: there is a large threshold field.

Polarisation measurement versus field at increasing temperature shows decrease of the threshold field, this fact is on one hand due to the increase of competition between antiferroelectric and ferroelectric order with temperature and on the other hand to the decrease of the viscosity with temperature (see figure 10).

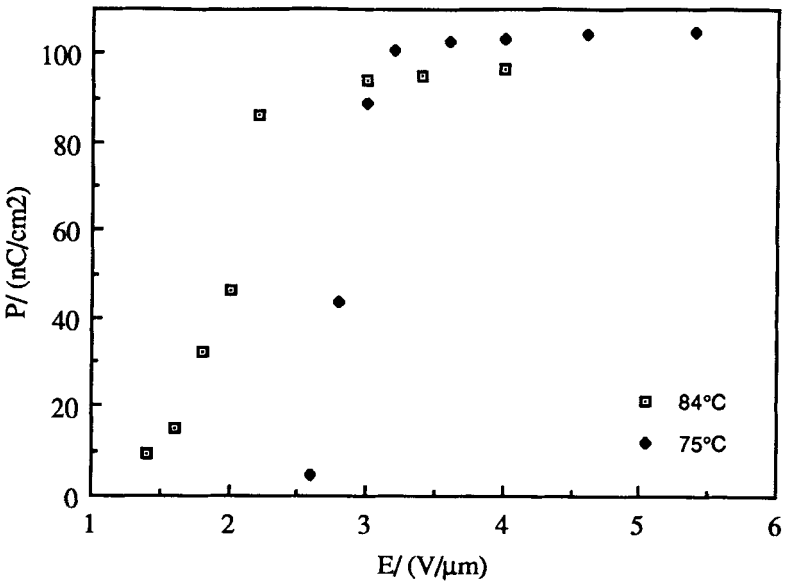

Figure 10:Polarisation versus field in SC*A phase at 75 and 84°C for n=10 (7.5 μm thick sample)

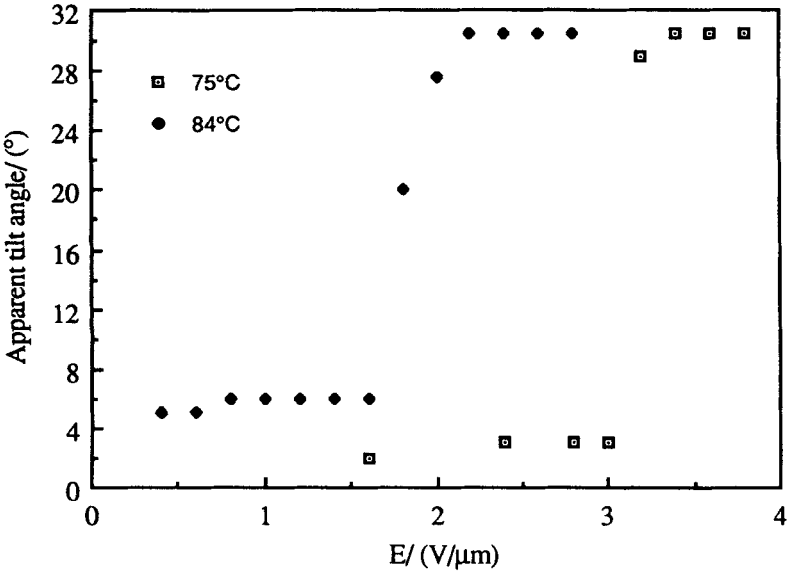

Figure 11:Apparent tilt angle versus field in SC*A phase at 75 and 84°C for n=10. (7.5 μm thick sample

This characteristic behaviour of $S_{C}*_{A}$ (threshold field) can easily be observed by the mesurement of the apparent tilt versus field, nevertheless below the threshold field we have measured a small induced angle probably due to electroclinic effect or surface anchoring effect (see figure 11).

$S_{I}*_{A}$ and S_{J} * phases

These phases are more ordered than the previous one, with a higher viscosity; consequently these phases require a higher field to reach polarisation saturation (more than 7V/μm in $S_{J}*$ phase)(see figure 12).

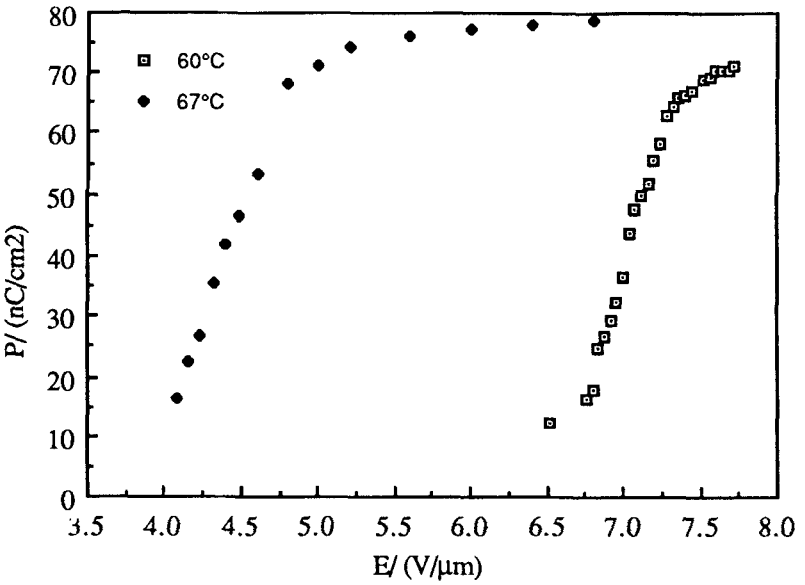

Figure 12: Polarisation versus field in $S_{J}*$ and $S_{I}*_{A}$ phase at 60 and 67°C for n=8. (5 μm thick sample)

An other fact confirming the great viscosity of this phases is the response time; which is approximatively ten times higher in $S_{J}*$ or $S_{I}*_{A}$ phases than in the $S_{CA}*$ phase (see figure 13 and 14).

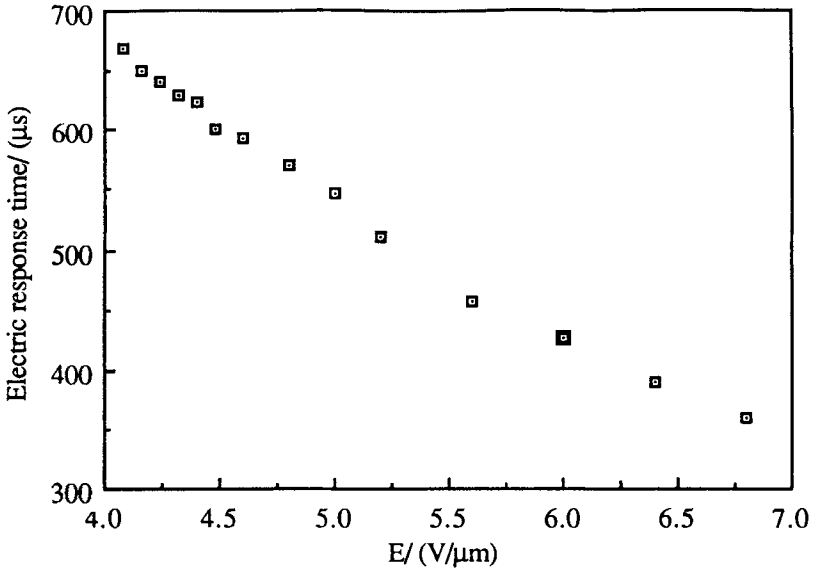

Figure13:Electric response time versus field in SI*A phase at 67°C for n=8. (5 μm thick sample)

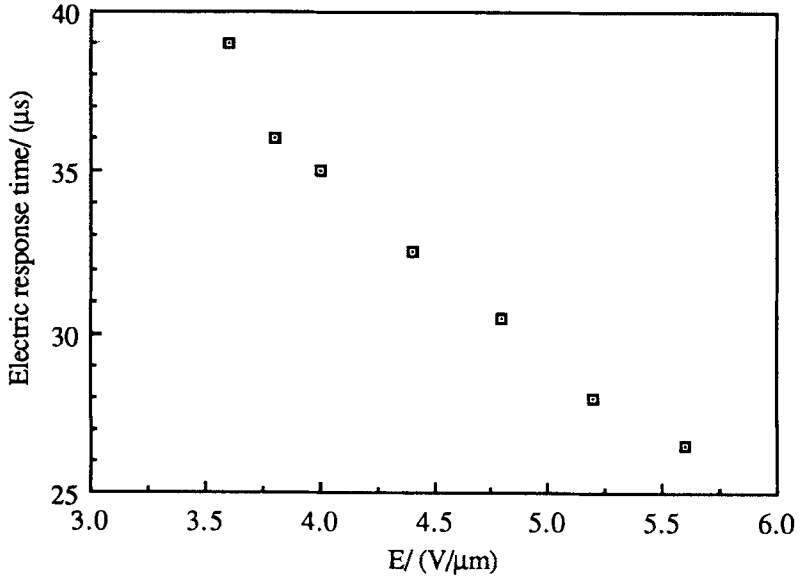

figure 14: electric response time versus field in SC*A phase at 75°C for n=10. (7.5 μm thick sample)

V PITCH MEASUREMENTS

The chirality seem to play a very important role in the understanding of the different tilted phases.

Thus we have used the n=8,9,10 tolane for helical pitch measurements. As previously described[14] we used prismatic cells with weak edge angle (less than 0.25 degree) oriented in the Grandjean-Cano texture; the required orientation is complanar (pseudo homeotropic).

A very good orientation is easely obtained in the S_C^* phase leading to the observation of a large number of equal width Grandjean-Cano steps thus allowing an accurate measurement of the pitch and of its temperature dependence. On the contrary the quality of the sample is rather poor in the $S_C^*{}_A$ phase; only one or two torn steps awailable.

The selective reflection of the light occuring in the S_C^* and $S_C^*{}_A$ phases allows a control of the pitch measurement values. For S_C^* phase, selective reflection correspond to $\lambda=np$ if the pitch is higher than 0.27 μm and $\lambda=2np$ when the pitch is lower than 0.27 μm (one can see a second complete visible spectrum near the transition $S_C^*/S_C^*{}_\alpha$ or S_C^*/S_A). Moreover selective reflection give an accurate value of the helical pitch in $S_C^*{}_A$ phase because of the bad quality of the steps; selective reflection in $S_C^*{}_A$ phase correspond to normal reflection with $\lambda=np$ ($\lambda=2np$ is prohibited because the period is half a pitch).

The direction of rotation of the helix can be determined by analizing the direction of the circularly polarized reflected light and/ or the sign of the rotatory power.

In the $S_C^*{}_{FI}$ phases no Grandjean-Cano steps could be obtained and we cannot provide any precise value of the pitch for this phase.

Thus we only provide a qualitative description of the variation of the helix. These have been established from complanar droplets in which one can observe: (i) equal thickness fringes, roughly parallel to the edge of the drop, tighten when the pitch decreases and move aside when the pitch increases. Disordered Grandjean-Cano threads cross more or less rapidely in the sample accounting for a more or less important temperature dependence of the twist.

The result are reported in figure 15,16,17. For n=9 compound pitch measurement is realised by selective reflection (reflective spectrometer) and Grandjean-Cano method, these two methods are in very good agreement (see figure16).

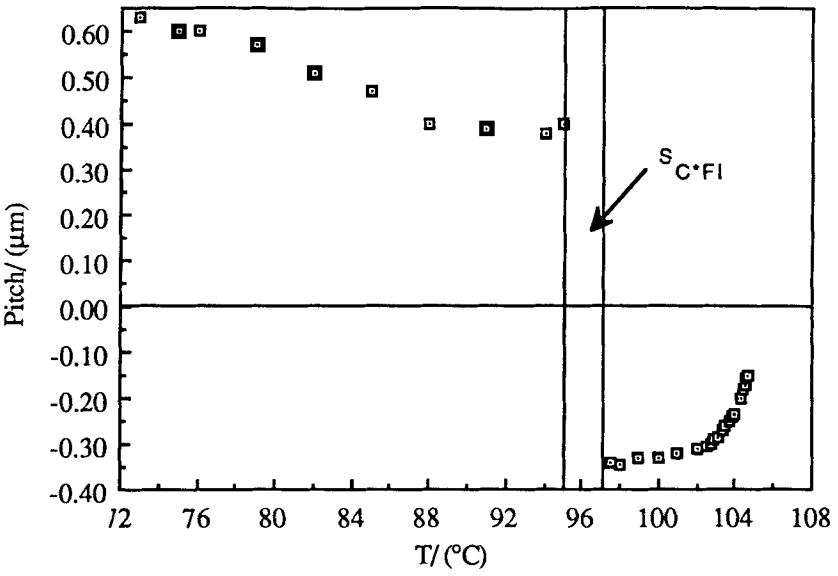

Figure 15: Temperature dependence of the helical pitch for n=8.

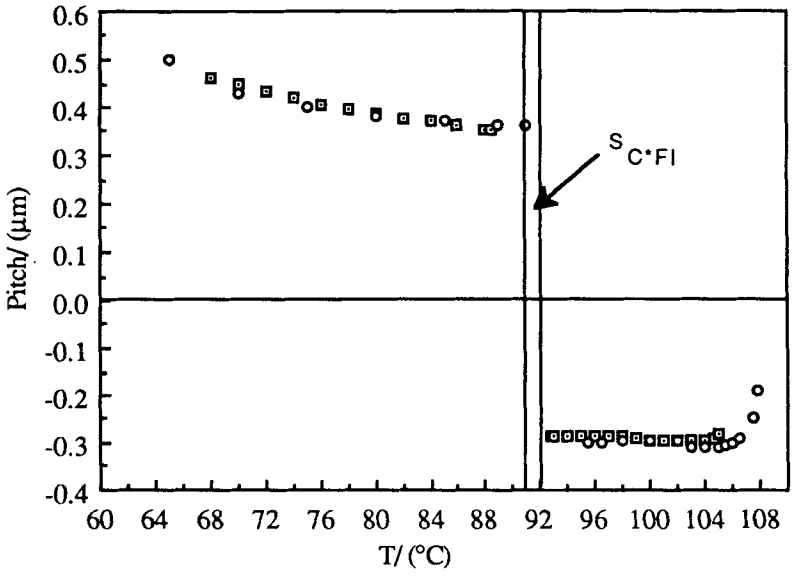

Figure 16: Temperature dependence of the helical pitch for n=9; Grandjean-Cano steps (squares) and selective reflection (circle).

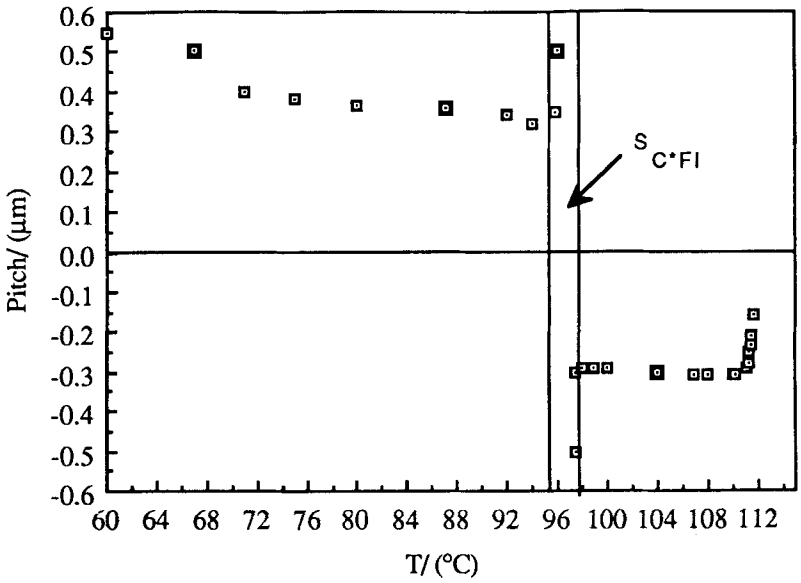

Figure 17: Temperature dependence of the helical pitch for n=10.

In addition the observation of complanar flat droplets allow the determination of the rotatory power: indeed the sense of the circularly polarized reflected light indicated that the helix is inversed between SC* and SC*A phase; this inversion occur somewhere in the SC*FI phase or between the two SC*FI phases (n=8).

General behaviour in SC*A phase is the same for the three compounds: the pitch is short (0,4μm) and decrease slowly with the temperature; and increase quickly at the SC*FI transition.

In SC* phase the pitch is very short too (0.3 μm), and decrease quickly at the SC*-SA transition (or SC*- SC*α transition).

We must underline that we have not been able to distinguish the SC*α phase in these pitch measurement experiments.The two SC*FI phases cannot be actually distinguish; but experimentaly the behaviour is the same for compound which have one or two SC*FI phases; nevertheless the pitch reversal occurs approximatively in the middle of SC*FI phase (n=9,10) and between the two SC*FI phase for n=8.

VI X-RAY SCATTERING

X-Ray diffraction experiments were performed to determine the layer thickness; only n=8 compound was studied. The liquid cristal was introduced in the isotropic phase in 1mm-diameter Lindeman capillaries. The sample was mounted on a Huber 2θ goniometer. The temperature was controled within a 0.01°C accuracy. The CuKα radiation of an 18kW rotating anode X-ray generator (Rigaku RU-200) was selected by a flat pyrolytic graphite (002) monochromator. The resulting horizontal instrumental resolution was 10^{-2} Å^{-1} (FWHM)The scattering profiles were fitted with the resolution function, the final accuracy on the bragg position was estimated about 10^{-3} Å^{-1} or equivalently about 0.25 Å in reciprocical space. The layer thickness is about 39.25 Å in the S_A phase (the molecular length is 44 Å). It decrease abrupty at the S_A-$S_C^*\alpha$, revealing the tilt of the molecular axis relative to the layer normal in the $S_C^*\alpha$ transition phase. The smectic period decreases regularly on cooling throughout the S_C^*, S_C^*FI1, S_C^*FI2, and S_C^*A phases and reaches a plateau at 88°C in the S_C^*A phase. The estimated tilt angle $\cos^{-1}(d/d_{SA})$ is then approximatly 19 degrees. Finally, the layers thickness increase abruptly on approaching the S_C^*A-S_I^*A transition (see figure 18). Eventually, the tilt angle of the S_I^*A phase is of order 13 degrees. We notice that the regular decrease of the layer thickness is somewhat broken in the S_C^*FI phases. The deviation is however not much larger than the experimental uncertainty.

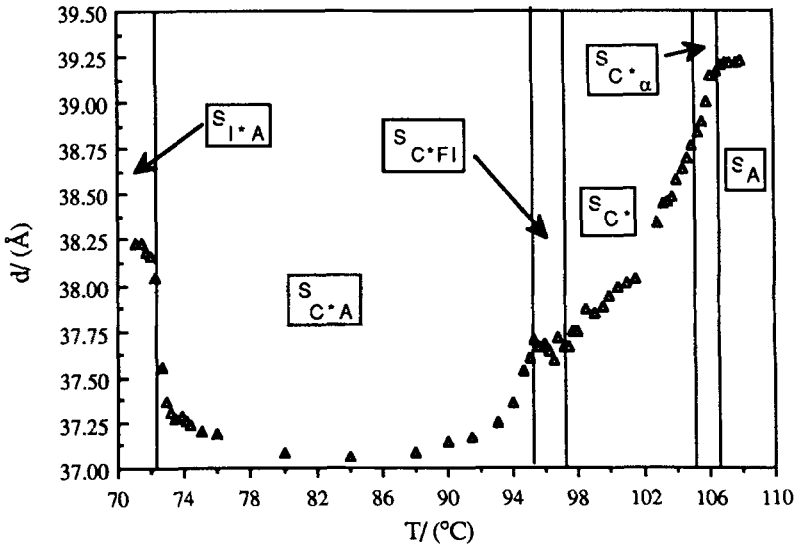

Figure 18:Layer spacing versus temperature as obtained from X-ray scans for n=8

EXPERIMENTAL

The infrared spectra were recorded using a Perkin-Elmer 783 spectrophotometer and the NMR spectra with a Bruker 270 MHz. All final compounds give satisfactory elemental analyses.

* Ethyl 4-tetrahydropyranyloxy-4'-methyloxycarbonyltolane 3:

In a 250 ml round bottomed flask were placed 4-tetrapyranyloxyphenylacetylene[15] (8 g; 0.04 mol), methyl 4-iodobenzoate (12.1 g; 0.044 mol), triphenylphosphine (TPP)(1 g; 3.8 mmol) in dipropylamine (120 ml) under nitrogen. The solution was stirred and heated in an oil bath at 30° C until complete dissolution. Then catalysts $PdCl_2$ (110 mg; 0.6 mmol) and $Cu(AcO)_2;H_2O$ (120 mg; 0.6 mmol) were added to this solution which was gradually heated to 100°C and maintained at this temperature for 4 h. After cooling to room temperature the salt was removed by filtration and washed well with ethyl acetate. The filtrate was evaporated and hydrolysed with concentrated hydrochloric acid (10 ml), water (100 ml) and crushed ice (100 g) and then extracted with ethyl acetate. The organic phase was dried over anhydrous Na_2SO_4, filtered and evaporated. The residue was filtered on silica gel with (9:1) heptane-ethyl acetate mixture. The pure compound was recrystallized in heptane. Yield: 10.8 g (77 per cent), m.p =122° C

^1H NMR: 1.6-2.1 (m, 6H of THP), 3.6 (m,1H of THP), 3.9 (m,1H of THP), 4 (s, 3H, *CH3*), 5.4 (t, 1H-O-CH-O), 6.6-8.1 (4d, 8H arom.)

IR (nujol): 2947, 1716, 1598, 1275, 835 cm^{-1}

*4-hydroxy-4'-methyloxycarbonyltolane 4

The tetrahydropyranyl derivative 3 (10.8 g) was dissolved in a CH_2Cl_2 (70 ml), CH_3OH (120 ml) mixture. To this solution was added 4-toluenesulfonic acid (PTSA)(0.3 g) and the mixture was stirred at room temperature for 1 h. The solvent was evaporated and the pure phenol was obtained by chromatography on slica gel with (8:2) heptane-ethyl acetate mixture. Yield: 7.5 g (90 per cent), m.p.=206° C

^1H NMR: 4 (s, 3H, CH_3), 6.9-8.1 (4d, 8H arom.), 8.9 (s, 1H, OH)

IR (nujol): 3413, 2931, 1690, 1272, 837 cm^{-1}

* 4-n-octyloxytolane-4'-carboxylic acid A

To the solution of KOH (0.60 g; 0.011 mol) in H_2O (5ml) and ethanol (30ml) was added phenol 4 (2.60 g; 0.01 mol). The solution was stirred at 50°C until complete

dissolution. Then 1-bromooctane (2.12 g; 0.011mol) was added dropwise and the solution was refluxed for 4 h. A 10% KOH solution was cautiously added to the mixture and the resulting solution was refluxed for 2 h. After cooling to room temperature, the solvent was removed on rotavapor and the residue was hydrolysed with concentrated hydrochloric (2ml) water and crushed ice. The solid was filtered and recrystallized in acetic acid. Yield 2.5 g (71 per cent) : C 229 S_C 235 N 258 I
IR (nujol): 2950, 1685, 1598, 1287 cm^{-1}

* (S)-4-(1-methylheptyloxycarbonyl)phenyl 4-n-octyloxytolane-4'-carboxylate.

To the solution of (S)-4-(1-methylheptyloxycarbonyl)phenol **B** (0.5 g;2 mmol) in CH_2Cl_2 (5 ml) was added dicyclohexylcarbodiimide (DCC) (0.45 g; 2.2 mmol), 4-dimethylaminopyridine (DMAP) (40 mg) and the acid **A** (0.77 g; 2.2 mmol). The resulting solution was stirred at room teperature overnight. The solution was filtered ,evaporated and chromatographied on silica gel with CH_2Cl_2 as eluent. The desired compound was recrystallized from absolute ethanol. Yied: 0. 78 g (64 per cent).
^1H NMR 0.85 (t, 6H, 2 CH_3), 1.24 (m, 18H, 9 CH_2), 1.3 (d, 3H, CH_3-CH), 1.4-1.9 (m, 4H, 2$CH_2\beta$), 4 (t, 2H, OCH_2), 5.15 (m, 1H, CH-CH_3), 6.8-8.2 (6d, 12H arom)
IR (nujol): 2930, 1736, 1711, 1283, 833 cm^{-1}

VII CONCLUSION

This new chiral series with tolane core described in this paper displays a complex smectic polymorphism: S_J*, S_I*A, S_C*A, S_C*FI, S_C*, S_C*α, S_A. DSC and optical observation indicate that two SC*FI phases can exist between the S_C* and S_C*A phases. The electrooptical study shows a different behaviour of each phases as a fonction of the field. One can note we observe a middle plateau of the polarisation at low field in the S_C*FI phase; nevertheless we observe exactly the same behaviour in the two S_C*FI phases. The helical pitch is short in S_C*A phase and S_C* phase with a change in the sense of the twist for this two phases. This change in the sense of the torsion occurs in the S_C*FI phase for the three compound (n=8,9,10). The evolution of layer thickness with temperature confirms that the S_C*α phase is tilted; and shows also a peculiarity in the S_C*FI temperature range.

REFERENCES:

1. J.W. Goodby, J.W. Waugh, M.A. Stein, S.M. Chin, E. Pindak, J.S. Patel, Nature, (Lond), 337, 449.
2. A.D.L. Chandani, Y. ouchi, H. Takezoe, A. Fukuda, K. Furukawa, A. Kishi, Jpn. Appl. Phy., 28, 1261, (1989).
3. A. Fukuda, Y. Takanishi, T. Isozaki, K. Ishikawa, H. Takezoe, Rewiew, (to be published).
4. G. Heppke, P. Kleineberg, D. Lotzsch, S. Mery, R. Shashidar, Mol. Liq. Cryst., 231, 257, (1993).
5. L. Dupont, M. Glogarova, J.P. Marcerou, H.T. Nguyen, C. Destrade, J. Phys. II, 1, 831, (1991)
6. T. Isozaki, K. Hiraoka, Y. Takanischi, H. Takezoe, Y. Suzuki, I. Kawamura, Liq. Cryst, 12, 59, (1992).
7. E. Gorecka, A.D.L. Chandani, Y. Ouchi, H. Takezoe, A. Fukuda, Jpn. J. Appl. Phys., 29, 131, (1990).
8. N. Okabe, Y. Suzuki, I. Kawamura, T. Isozaki, H. Takezoe, A. Fukuda, Jpn. J. Appl. Phys., 31, L793, (1990).
9. H.T. Nguyen, J.C. Rouillon, P. Cluzeau, G. Sigaud, C. Destrade, N. Isaert, Liq. Cryst., (accepted).
10. I. Nishiyama, E. Chin, J.W. Goodby, J. Mater. Chem., 3, 161, (1993).
11. Y. Galerne, L. Liebert, Phys. Rev. Lett., 64, 906, (1990).
12. Y. Galerne, L. Liebert, Phys. Rev. Lett., 66, 2891, (1991).
13. C. Bahr, D. Fliegner, C.J. Booth, J.W. Goodby, Euro. Phys. Lett., 26, 539, (1994).
14. M. Brunet, N. Isaert, Ferroelectrics, 84, 25, (1988).
15. A. Bouchta, H.T. Nguyen, M.F. Achard, F. Hardouin, C. Destrade, Liq. Cryst.,12, 575, (1992).